Received: 19 November 2022 | Revised: 1 February 2024 | Accepted: 17 February 2024

DOI: 10.1111/cas.16128

Cancer Science WILEY

ORIGINAL ARTICLE

Upregulation of HLA-II related to LAG-3^{+}CD4^{+} T cell infiltration is associated with patient outcome in human glioblastoma

Wenli Guo[1,2] | Daijun Peng[1] | Yuee Liao[1] | Lei Lou[1] | Moran Guo[3] | Chen Li[4] | Wangyang Yu[4] | Xiaoxi Tian[1] | Guohui Wang[1] | Ping Lv[5] | Jing Zuo[6] | Haitao Shen[2,7] | Yuehong Li[1,2]

[1]Department of Pathology, The Second Hospital, Hebei Medical University, Shijiazhuang, China

[2]Laboratory of Pathology, Hebei Medical University, Shijiazhuang, China

[3]Department of Neurology, Second Hospital of Hebei Medical University, Shijiazhuang, China

[4]Department of Neurosurgery, Second Hospital of Hebei Medical University, Shijiazhuang, China

[5]Department of Pharmacology, Hebei Medical University, Shijiazhuang, China

[6]Department of Oncology, The Fourth Hospital of Hebei Medical University, Shijiazhuang, China

[7]Hebei Collaborative Innovation Center of Tumor Microecological Metabolism Regulation, Hebei University, Baoding, China

Correspondence
Yuehong Li, Department of Pathology, The Second Hospital, Hebei Medical University, No. 215, Heping West Road, Xinhua District, Shijiazhuang 050004, China.
Email: liyuehong1993@126.com

Haitao Shen, Laboratory of Pathology, Hebei Medical University, No. 361, East Zhongshan Road, Shijiazhuang 050017, China.
Email: haitaoshen78@hotmail.com

Funding information
National Natural Science Foundation of China, Grant/Award Number: 31570894, 81670939 and 81672706; Science and Technology Program of Hebei Province, China, Grant/Award Number: 216Z7707G and 216Z7701G; Natural Science Foundation of Hebei Province, China, Grant/Award Number: H2019206709, H2021206351 and H2022206551

Abstract

Glioblastoma (GBM) is the most common malignant diffuse glioma of the brain. Although immunotherapy with immune checkpoint inhibitors (ICIs), such as programmed cell death protein (PD)-1/PD ligand-1 inhibitors, has revolutionized the treatment of several cancers, the clinical benefit in GBM patients has been limited. Lymphocyte-activation gene 3 (LAG-3) binding to human leukocyte antigen-II (HLA-II) plays an essential role in triggering CD4^{+} T cell exhaustion and could interfere with the efficiency of anti-PD-1 treatment; however, the value of LAG-3–HLA-II interactions in ICI immunotherapy for GBM patients has not yet been analyzed. Therefore, we aimed to investigate the expression and regulation of HLA-II in human GBM samples and the correlation with LAG-3^{+}CD4^{+} T cell infiltration. Human leukocyte antigen-II was highly expressed in GBM and correlated with increased LAG-3^{+}CD4^{+} T cell infiltration in the stroma. Additionally, HLA-II^{High}LAG-3^{High} was associated with worse patient survival. Increased interleukin-10 (IL-10) expression was observed in GBM, which was correlated with high levels of HLA-II and LAG-3^{+} T cell infiltration in stroma. HLA-II^{High}IL-10^{High} GBM associated with LAG-3^{+} T cells infiltration

Abbreviations: APC, antigen-presenting cell; Arg-1, Arginase-1; CGGA, Chinese Glioma Genome Atlas; FCM, flow cytometry; GBM, glioblastoma; GEPIA, Gene Expression Profiling Interaction Analysis; GFAP, glial fibrillary acidic protein; HLA, human leukocyte antigen; ICI, immune checkpoint inhibitor; IHC, immunohistochemistry; IL-10, interleukin-10; LAG-3, lymphocyte-activation gene 3; OS, overall survival; PD-1, programmed cell death protein 1; PD-L1, programmed cell death ligand 1; PGE2, prostaglandin E2; PMA, phorbol 12-myristate 13-acetate; ssGSEA, single-sample gene set enrichment analysis; sTNFR:Fc, soluble TNF receptor:Fc fusion protein; TCGA, The Cancer Genome Atlas; TIL, tumor-infiltrating lymphocyte; TIM-3, T cell immunoglobulin domain and mucin domain-3; TNF-α, tumor necrosis factor-α.

Wenli Guo and Daijun Peng contributed equally to this work.

synergistically showed shorter overall survival in patients. Combined anti-LAG-3 and anti-IL-10 treatment inhibited tumor growth in a mouse brain GL261 tumor model. In vitro, $CD68^+$ macrophages upregulated HLA-II expression in GBM cells through tumor necrosis factor-α (TNF-α). Blocking TNF-α-dependent inflammation inhibited tumor growth in a mouse GBM model. In summary, T cell–tumor cell interactions, such as LAG-3–HLA-II, could confer an immunosuppressive environment in human GBM, leading to poor prognosis in patients. Therefore, targeting the LAG-3–HLA-II interaction could be beneficial in ICI immunotherapy to improve the clinical outcome of GBM patients.

KEYWORDS
glioblastoma, HLA-II, IL-10, immune checkpoint inhibitor, LAG-3

1 | INTRODUCTION

Glioblastoma is the most common malignant diffuse glioma and is a highly aggressive brain tumor. With standard treatments, such as surgery, temozolomide chemotherapy, radiotherapy, and corticosteroid therapy, the median survival rates for GBM patients remain low.[1] Although immunotherapy utilizing ICIs, such as PD-1/PD-L1 inhibitors, has revolutionized the treatment of several cancers, its clinical benefit in GBM patients is limited.[2] In GBM, the lack of clinically meaningful responses to ICI has been attributed to the specialized immune environment of the brain, which includes mechanical obstruction at the blood–brain barrier, T cell exhaustion, and a generally immunosuppressive environment.[3] A comprehensive understanding of ICI regulation within the brain tumor could reveal potential methods for improving the efficiency of immunotherapeutic interventions. Therefore, preventing cancer immunosuppression by targeting ICI could provide a suitable strategy for immunotherapy in GBM patients.[1,4,5]

Lymphocyte-activation gene 3 is a well-known immune checkpoint, and many studies have concluded that LAG-3, PD-1, or TIM-3 are markers of T cell exhaustion in glioma and are associated with poor prognosis.[4,6,7] Lymphocyte-activation gene 3 in activated T cells primarily binds to MHC-II molecules in APCs, reducing T cell proliferation and increasing T cell exhaustion.[8–11] The benefits of anti-LAG-3 therapy in different malignancies have been reported.[12,13] Upregulation of LAG-3 limits the antitumor activity of PD-1/PD-L1 inhibitors by attenuating T cell activation and preventing tumor cell destruction.[14,15] A preclinical study using a mouse model for glioma showed that treatment with anti-LAG-3 Abs, either alone or in combination with a PD-1 inhibitor, resulted in prolonged survival.[16] The prognostic value of LAG-3 expression in solid tumors has been monitored as an important immune checkpoint[17]; however, the role of LAG-3 ICI therapy in GBM remains to be elucidated.

The MHC, encoding the major histocompatibility antigens of animals, is also known as the HLA in humans. Human leukocyte antigen-II is encoded by three different loci: HLA-DR, HLA-DQ, and HLA-DP.[18,19] Human leukocyte antigen-II expression in tumor cells is a predictive biomarker of the preferred anti-PD-1 therapy in melanoma, Hodgkin's lymphoma, and lung adenocarcinoma.[20–22] Lymphocyte-activation gene 3 can directly and specifically interact with HLA-II heterodimers, providing new insights into the mechanism by which LAG-3 initiates T cell inhibition.[23] Human leukocyte antigen-II has been shown to inhibit T cell antitumor activity in cutaneous melanoma cells through their LAG-3 receptor.[24] Lymphocyte-activation gene 3 and its ligand HLA-II are highly expressed in high-risk uveal melanoma and could be a target for adjuvant immunotherapy.[25] Lymphocyte-activation gene 3 binding to HLA-II plays an essential role in triggering $CD4^+$ T cell exhaustion and might interfere with the efficiency of anti-PD-1 treatment in classical Hodgkin's lymphoma.[26] However, the expression of HLA-II in human GBM requires elucidation, and the value of LAG-3–MHC-II interactions in ICI immunotherapy for patients with GBM has not been analyzed.

We, therefore, aimed to explore the expression of HLA-II and its correlation with $LAG\text{-}3^+CD4^+$ T cell infiltration in human GBM samples. Moreover, we investigated the mechanism involved in the regulation of HLA-II in GBM cells in vitro. This study provides novel insights into the theoretical basis for the development of LAG-3–MHC-II immune-related intervention targets for GBM.

2 | MATERIALS AND METHODS

2.1 | Materials

Information regarding materials is provided in Appendix S1.

2.2 | Human case selection

Fifty-one cases of paraffin-embedded GBM specimens and 27 cases of paraffin-embedded normal brain specimens were archived in the Department of Pathology, Second Hospital of Hebei Medical University (collected between January 2011 and August 2016) with a median follow-up period of 18 months (range, 8–27 months). Clinical

histopathological data of patients and information on OS of patients were collected until death or the end of the investigation. Twenty-one cases of fresh GBM and paired paraneoplastic brain tissues for protein and RNA extraction, and 30 cases of frozen GBM specimens and 6 cases of frozen control brain specimens for immunofluorescence staining were provided by the Department of Neurosurgery, Second Hospital of Hebei Medical University. All the cases above were diagnosed by at least two board-certified neuropathologists according to the 2021 WHO guidelines. The expression of IDH1-R132H protein was determined by IHC. The normal brain tissues used as negative controls were obtained from paraneoplastic brain tissues who underwent glioma surgery or nontumor patients who underwent traumatic brain injury decompression surgery. Patients who agreed to have their samples used for scientific research provided written informed consent. The study was approved by the Ethics Committee of Hebei Medical University, and the treatment of the collected data and specimens was in accordance with ethical and legal standards.

The Cancer Genome Atlas of glioma and survival data was downloaded from TCGA: Oncomine database (https://www.oncomine.org) and GEPIA (http://gepia.cancer-pku.cn/) online platforms. Furthermore, 301 glioma samples were downloaded from the CGGA (http://cgga.org.cn/).

2.3 | Immunofluorescence staining

The tumor tissues from the GBM patients were immersed in 4% formalin, embedded in an optimal cutting temperature compound, and then subjected to immunofluorescence staining per the manufacturer's protocol.[27]

2.4 | Immunohistochemical score in human GBM

The IHC staining was processed as previously described.[27] The degree of immunostaining was scored independently by stained tumor cells and staining intensity according to a previous study.[27] The details of score are provided in Appendix S1.

2.5 | Mouse s.c. tumor model

Female C57BL/6 mice (6–8 weeks; 18–20 g) were maintained in specific pathogen-free conditions at animal facilities. Experimental protocols were approved by the Institutional Animal Care and Use Committee of Hebei Medical University. All animals were managed and treated according to the guidelines of Hebei Medical University. Briefly, C57BL/6 mice were inoculated with 2×10^6 GL261 tumor cells s.c. into the flank region. When visible tumors appeared (day 12), those mice were divided into four groups, and injected with anti-LAG-3 or anti-IL-10 or combined anti-LAG-3 and anti-IL-10 (10 μg/kg i.p., given four times). In some experiments, the mice were injected with sTNFR:Fc every 2 days (100 mg/kg body weight i.p., given four times). Another 10 days later, the animals were killed, and the tumor weight derived from each group was measured at day 22. The tumor volumes were measured every 2 days from day 12 to 22 using the following formula:

$$V = 0.5 \times (\text{length}) \times (\text{width})^2.$$

2.6 | Cell culture and treatment

Human U87, U251, and THP-1 cells were purchased from Peking Union Cell Resource Center. U87 and U251 were cultured in DMEM containing 10% FBS and penicillin/streptomycin at 37°C and 5% CO_2 humidified atmosphere. All experiments were carried out with mycoplasma-free cells. U87 and U251 cells were treated with different doses of TNF-α, and the expression of HLA-II was measured by FCM and western blot analysis. THP-1 cells were cultured in RPMI-1640 supplemented with antibiotics and 10% FCS and matured by PMA (Sigma). To differentiate into M0 macrophages, THP-1 cells (3.5×10^5 cells/well) were induced by 50 ng/mL PMA for 48 h as previously described. The obtained M0 cells were treated with lipopolysaccharide by 100 ng/mL to induce their differentiation into M1 macrophages. The conditioned medium from M1 cells was collected, with or without blocking by 15 μg/mL anti-TNF-α, and then used to stimulate U87 or U251 cells for 24 h. The HLA-DP or HLA-DQ expression in U87 or U251 cells was quantified through western blot assays. The experiments were undertaken at least three times.

2.7 | Western blot analyses

Tissues or cells were harvested and homogenized in 50 μL lysis buffer (50 mM Tris–HCl pH 7.5, 150 mM NaCl, 2 mM EDTA, 1% Triton X-100, cocktail) as previously described.[27] The experiments were processed according to a previous study.[27]

2.8 | Quantitative real-time PCR

The experiments were processed according to a previous study.[27] The details of scores are provided in Appendix S1. The primer sequences used for PCR amplification are shown in Table 1.

2.9 | Statistical analysis

The results were analyzed using SPSS 24.0 (IBM Corp.). Data from clinical samples were analyzed using the Mann–Whitney *U*-test and Spearman's correlation. Overall survival was measured from the date of operation to the date of death, or the last clinical follow-up time before September 2022, according to the Kaplan–Meier method. The log-rank test was used to compare the survival distribution. All in vitro data were tested using one-way ANOVA. Data are expressed

TABLE 1 Primer sets used for quantitative real-time PCR.

Human	Forward primer	Reverse primer
HLA-DP	AGGCAGCATTCAAGTCCGAT	GGGGGTCATTTCCAGCATCA
HLA-DQ	ATGTCCAGTAACACAGAAGCCA	AAGGGCAGACGGTATCCATTA
IL-10	GCTCTTGCAAAACCAAACCACA	TCTCGAAGCATGTTAGGCAG
TGF-β	CGACTCGCCAGAGTGGTTAT	CGGTAGTGAACCCGTTGATGT
PGE2 (PTGS2)	CTGCGCCTTTTCAAGGATGG	CCCCACAGCAAACCGTAGAT
TNF-α	TGTCCCTTTCACTCACTGGC	CATCTTTTGGGGGAGTGCCT
IL-1β	TCCCCAGCCCTTTTGTTGAG	GGAGCGAATGACAGAGGGTT
IL-6	TGCAATAACCACCCCTGACC	GTGCCCATGCTACATTTGCC

Abbreviations: HLA, human leukocyte antigen; IL, interleukin; PGE2, prostaglandin E2; TGF-β, transforming growth factor-β; TNF-α, tumor necrosis factor-α.

as mean ± SD obtained from at least three independent experiments. Data were analyzed using the nonparametric Mann–Whitney *U*-test (significance level $p < 0.05$).

3 | RESULTS

3.1 | Expression of HLA-II in human GBM

Among the 552 specimens from TCGA (542 cases of GBM and 10 cases of normal brain tissues), the mRNA expression levels of HLA-DP, HLA-DQ, and HLA-DR were higher in GBM than in normal brain (Figure 1A). The CGGA datasets showed the mRNA expression levels of HLA-DP, HLA-DQ, and HLA-DR in GBM WHO IV were higher than those in WHO II (Figure S1A). The HLA-DQ and HLA-DR expression was not associated with shorter OS, whereas HLA-DP was associated with shorter OS in patients with GBM (Figure 1B).

To further validate the findings from TCGA and CGGA, we explored HLA-II expression in 51 cases of paraffin-embedded GBM specimens and 27 control specimens. Immunohistochemical staining showed positive expression of HLA-DP, HLA-DQ, and HLA-DR in the GBM (Figure 1C). The expression of HLA-DP and HLA-DQ was significantly higher in human GBM than in the control (Figure 1D,E). There was no difference in HLA-DR expression between GBM and control (Figure 1F). In addition, a comparison of 21 pairs of fresh GBM and adjacent control samples revealed that HLA-DP and HLA-DQ were upregulated in GBM (Figures 1G,H and S1C). We also detected HLA-DP and HLA-DQ expression in $GFAP^+$ GBM cells using immunofluorescence staining (Figure S1D,F). The numbers of $HLA\text{-}DP^+GFAP^+$ and $HLA\text{-}DQ^+GFAP^+$ cells were significantly higher in human GBM than in the control (Figure S1E,G). Using seven pairs of fresh GBM and adjacent control samples, we also detected HLA-II expression in human $GFAP^+$ GBM cells by FCM staining. Flow cytometry analysis indicated the percentage of $HLA\text{-}II^+GFAP^+$ cells in human GBM was higher than in control brain tissues (Figure S2A,B). However, high levels of HLA-II were not associated with OS according to HLA-II expression in paraffin-embedded GBM specimens (Figure 1I–K), suggesting that HLA-II in tumor cells might not be an independent factor in the prognosis of GBM patients.

3.2 | Expression of HLA-II is related to infiltration of $LAG\text{-}3^+CD4^+$ T cells in GBM

Based on TCGA, the mRNA expression of LAG-3, TIM-3, and PD-1 was significantly higher in GBM than in controls (Figure 2A). The CGGA datasets showed the mRNA expression levels of LAG-3, TIM-3, and PD-1 in GBM WHO IV were higher than those in WHO II (Figure S3A). The TCGA from the Oncomine and GEPIA databases as well as CGGA databases showed that high mRNA expression of LAG-3, TIM-3, and PD-1 was not associated with OS in GBM patients (Figure S3B–D). In seven pairs of fresh GBM and adjacent control samples, FCM staining showed the percentage of $LAG\text{-}3^+CD4^+$ T cells in human GBM was higher than that in control brain tissues (Figure S2C,D). Based on IHC staining in 51 cases of paraffin-embedded GBM specimens, we found LAG-3, TIM-3, and PD-1 were mainly expressed in tumor stroma (Figure S4A–C). The infiltration of $LAG\text{-}3^+$, $TIM\text{-}3^+$, and $PD\text{-}1^+$ cells in GBM stroma was greater than that in controls (Figure S4D–F). The expression of LAG-3, TIM-3, and PD-1 was upregulated in infiltrating lymphocytes. To analyze patient survival, we used the median expression levels of $LAG\text{-}3^+$, $TIM\text{-}3^+$, and $PD\text{-}1^+$ cells as cut-off points to divide the GBM into high- and low-expression groups. High expression of LAG-3, TIM-3, and PD-1 was not associated with shorter OS of patients with GBM (Figure S4G–I).

FIGURE 1 Expression of human leukocyte antigen-II (HLA-II) molecules in human glioblastoma (GBM). (A) Evaluation of HLA-II expression from The Cancer Genome Atlas (TCGA). (B) Association between HLA-DP, HLA-DQ, and HLA-DR expression and survival follow-up time in TCGA datasets. (C) Immunohistochemical (IHC) images indicate the expression of HLA-II in paraffin GBM specimens. (D–F) Comparison of HLA-II molecules expression in control and GBM samples was analyzed (51 cases of GBM and 27 control tissues). (G, H) Twenty-one pairs of fresh tumor tissues and peritumoral brain tissues were collected, and the expression of HLA-II was measured by western blot. The comparison of HLA-II between GBM (T) and control (N) tissues is shown ($n = 21$). (I–K) Overall survival was measured according to the expression of HLA-II in paraffin-embedded GBM ($n = 46$).

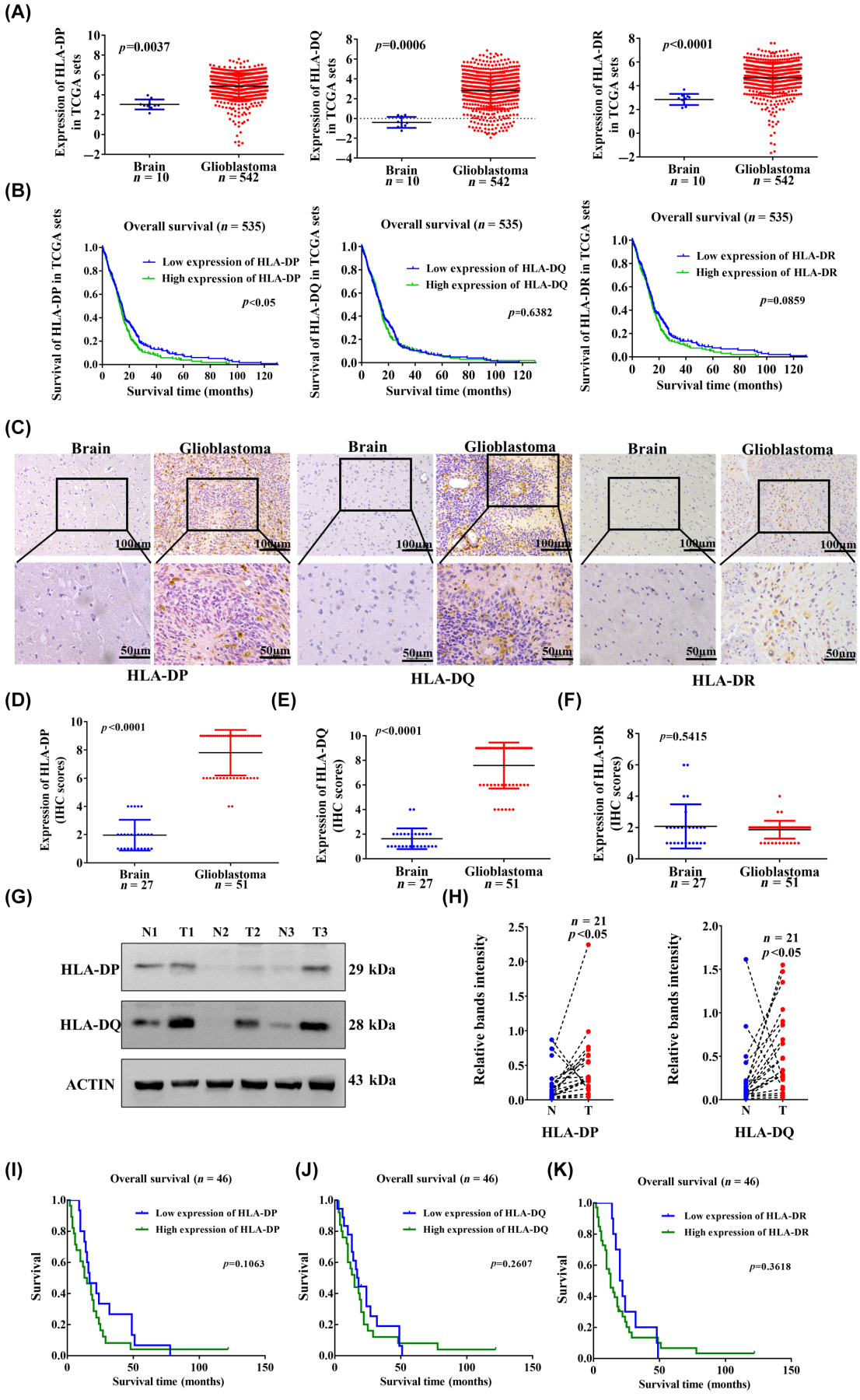
(A)
Expression of HLA-DP in TCGA sets
p=0.0037
Brain n = 10
Glioblastoma n = 542
Expression of HLA-DQ in TCGA sets
p=0.0006
Expression of HLA-DR in TCGA sets
p<0.0001
(B)
Overall survival (n = 535)
Survival of HLA-DP in TCGA sets
Low expression of HLA-DP
High expression of HLA-DP
p<0.05
Survival time (months)
Survival of HLA-DQ in TCGA sets
Low expression of HLA-DQ
High expression of HLA-DQ
p=0.6382
Survival of HLA-DR in TCGA sets
Low expression of HLA-DR
High expression of HLA-DR
p=0.0859
(C)
Brain
Glioblastoma
100μm
50μm
HLA-DP
HLA-DQ
HLA-DR
(D)
Expression of HLA-DP (IHC scores)
p<0.0001
Brain n = 27
Glioblastoma n = 51
(E)
Expression of HLA-DQ (IHC scores)
p<0.0001
(F)
Expression of HLA-DR (IHC scores)
p=0.5415
(G)
N1 T1 N2 T2 N3 T3
HLA-DP
29 kDa
HLA-DQ
28 kDa
ACTIN
43 kDa
(H)
Relative bands intensity
n = 21
p<0.05
N T
HLA-DP
HLA-DQ
(I)
Overall survival (n = 46)
Survival
Low expression of HLA-DP
High expression of HLA-DP
p=0.1063
Survival time (months)
(J)
Low expression of HLA-DQ
High expression of HLA-DQ
p=0.2607
(K)
Low expression of HLA-DR
High expression of HLA-DR
p=0.3618

We collected 30 frozen GBM specimens and six frozen control specimens for immunofluorescence staining, and detected $CD4^+LAG\text{-}3^+$, $CD3^+TIM\text{-}3^+$, and $CD3^+PD\text{-}1^+$ T cell infiltration in the tumor stroma (Figure 2B). The infiltration of $CD4^+LAG\text{-}3^+$, $CD3^+TIM\text{-}3^+$, and $CD3^+PD\text{-}1^+$ T cells was higher in GBM specimens than those in the controls (Figure 2C). Immunofluorescence images indicated the infiltration of $LAG\text{-}3^+CD4^+$ cells in tumor stroma, which was associated with HLA-DP and HLA-DQ expression in the same field (Figures 2D and S5). Glioblastoma patients with high HLA-DP expression showed increased $CD4^+LAG\text{-}3^+$ T cell infiltration (Figure 2E). The number of $CD4^+LAG\text{-}3^+$ T cells closely correlated with HLA-DP expression based on immunofluorescence staining (Figure 2F). In seven pairs of fresh GBM and adjacent control samples, FCM staining showed the percentage of $LAG\text{-}3^+CD8^+$ T cells in human GBM was higher than that in control brain tissues (Figure S2C,E). Immunofluorescence staining indicated that the infiltration of $CD8^+LAG\text{-}3^+$ T cells was higher in GBM specimens than in controls (Figure S6A,B). However, the number of $CD8^+LAG\text{-}3^+$ T cells was not correlated with HLA-DP or HLA-DQ expression based on immunofluorescence staining (Figure S6C,D). Thus, the results clearly indicate that increased HLA-II expression is related to the infiltration of $LAG\text{-}3^+CD4^+$ T cells in GBM.

In addition, data from TCGA (Figure S7A) and CGGA (Figure S7B) showed that HLA-DP/HLA-DQ upregulation was positively correlated with LAG-3 expression in GBM. Immunohistochemical staining showed that positive expression of HLA-DP, HLA-DQ, CD4, and LAG-3 was observed in the same field of paraffin-embedded GBM samples (Figure S7C). Based on both HLA-II and LAG-3 expression in paraffin-embedded GBM specimens, the case numbers of $HLA\text{-}II^{High}LAG\text{-}3^{High}$ or $HLA\text{-}II^{Low}LAG\text{-}3^{Low}$ is shown in Table 2. Spearman's correlation analysis showed that HLA-DP and HLA-DQ expression was positively correlated with $LAG\text{-}3^+$ lymphocyte infiltration in 51 cases of GBM samples (Figure S7D,E). Glioblastoma patients with high HLA-DP expression showed increased $LAG\text{-}3^+$ T cell infiltration (Figure S7F,G). We analyzed the OS of patients according to $HLA\text{-}DP^{High}LAG\text{-}3^{High}$ versus $HLA\text{-}DP^{Low}LAG\text{-}3^{Low}$. Patients with $HLA\text{-}DP^{Low}LAG\text{-}3^{Low}$ had a longer OS than those with $HLA\text{-}DP^{High}LAG\text{-}3^{High}$ (Figure 2G). Patients with $HLA\text{-}DQ^{High}LAG\text{-}3^{High}$ were not associated with poor survival (Figure 2H). Interestingly, patients with $HLA\text{-}DP^{Low}LAG\text{-}3^{Low}$ had a better prognosis (Figure 2I). Therefore, $HLA\text{-}DP^{High}$ and $LAG\text{-}3^{High}$ are independent factors, which could confer an immunosuppressive environment in GBM.

3.3 | Human leukocyte antigen-II is related to IL-10 expression in GBM

Based on TCGA, the mRNA expression of anti-inflammatory cytokines IL-10, TGF-β, and PGE2 and pro-inflammatory cytokines IL-1β and IL-6 was upregulated in GBM compared to that in normal brain tissues (Figure S8A). We isolated 21 fresh GBM samples, and measured HLA-II and cytokine expression. The expression of HLA-DP was upregulated in 13 cases of GBM samples, which showed upregulation of IL-10, TNF-α, and PGE2 (Figures 3A,B and S8B). Upregulation of HLA-DQ was observed in 14 cases of GBM samples, which showed high expression of IL-10 and IL-6 (Figures 3A,C and S8B).

Data from TCGA and CGGA showed HLA-DP/DQ expression was also correlated with IL-10 expression in GBM (Figure S8C,D). Immunohistochemical staining showed positive expression of IL-10 in 51 cases of paraffin-embedded GBM specimens, and IL-10 expression was increased in GBM compared to that in control specimens (Figure 3D,E). A trend toward worse OS was indicated in patients with IL-10 upregulation (Figure 3F). In paraffin-embedded GBM specimens, IHC images showed positive staining of HLA-DP, HLA-DQ, and IL-10 in the same field (Figure 3G). The case numbers of $HLA\text{-}II^{high}IL\text{-}10^{high}$ or $HLA\text{-}II^{low}IL\text{-}10^{low}$ are shown in Table 2. Both HLA-DP and HLA-DQ expression was positively correlated with IL-10 upregulation (Figure 3H,I). Based on both HLA-II and IL-10 expression in paraffin-embedded GBM specimens, multivariate analysis indicated the patients with $HLA\text{-}II^{Low}IL\text{-}10^{Low}$ had a longer OS than those with $HLA\text{-}II^{High}IL\text{-}10^{High}$ (Figure 3J,K).

3.4 | Blocking of LAG-3 and IL-10 inhibits GBM progression

We also analyzed the relationship between IL-10 expression and $LAG\text{-}3^+$ cell infiltration in 51 paraffin-embedded GBM specimens. An increased number of $LAG\text{-}3^+$ cells was positively correlated with IL-10 upregulation (Figure 4A). Furthermore, we divided the paraffin-embedded GBM samples into four groups based on the combined expression of HLA-II and IL-10: $HLA\text{-}II^{High}IL\text{-}10^{High}$, $HLA\text{-}II^{High}IL\text{-}10^{Low}$, $HLA\text{-}II^{Low}IL\text{-}10^{Low}$, and $HLA\text{-}II^{Low}IL\text{-}10^{High}$ to analyze $LAG\text{-}3^+$ cell infiltration. The number of $LAG\text{-}3^+$ cells in $HLA\text{-}DP/DQ^{High}IL\text{-}10^{High}$ GBM stroma was significantly higher than that in $HLA\text{-}DP/DQ^{Low}IL\text{-}10^{Low}$ GBM stroma (Figure 4B,C). The case

FIGURE 2 Human leukocyte antigen-II (HLA-II) expression is related to the infiltration of lymphocyte-activation gene 3 $(LAG\text{-}3)^+CD4^+$ T cells in glioblastoma (GBM). (A) Evaluation of LAG-3, T cell immunoglobulin domain and mucin domain-3 (TIM-3), and programmed cell death protein 1 (PD-1) expression from the TCGA. (B) Thirty cases of frozen GBM samples and six cases of control brain samples were collected, and immunofluorescence staining showed that LAG-3 was colocalized with CD4, and TIM-3 and PD-1 were colocalized with CD3 in the tumor stroma. White arrows indicate colocalized cells. (C) The number of $LAG\text{-}3^+CD4^+$, $TIM\text{-}3^+CD3^+$, and $PD\text{-}1^+CD3^+$ cells in GBM and control samples is shown ($p < 0.05$). (D) Thirty cases of frozen GBM and six control samples were collected, and immunofluorescence staining indicated that $LAG\text{-}3^+CD4^+$ cells in the tumor stroma, which is associated with HLA-DP and HLA-DQ expression. White arrows indicate colocalized cells. (E) The correlation between number of $CD4^+LAG\text{-}3^+$ T cell infiltration and HLA-DP is shown. (F) The correlation between HLA-DP expression and the number of $CD4^+LAG\text{-}3^+$ T cells is shown. (G, H) Based on both HLA-II and LAG-3 expression in paraffin-embedded GBM specimens, overall survival was analyzed according to $HLA\text{-}II^{High}LAG\text{-}3^{High}$ and $HLA\text{-}II^{Low}LAG\text{-}3^{Low}$ ($n = 46$). (I) Kaplan–Meier curves for survival outcomes of patients are shown according to low expression of HLA-DP and LAG-3 ($n = 46$).

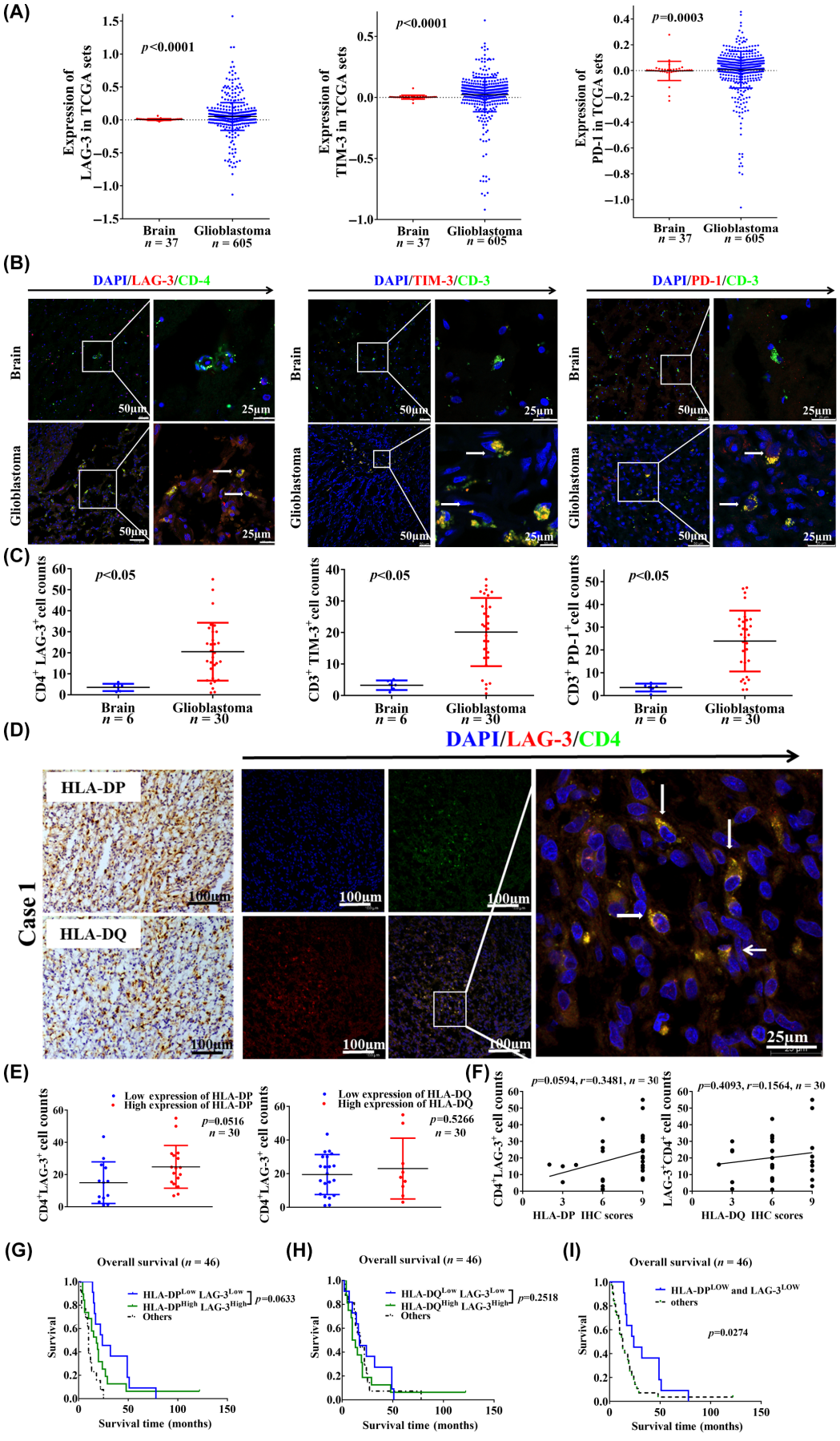
(A)
Expression of LAG-3 in TCGA sets
p<0.0001
Brain n = 37
Glioblastoma n = 605
Expression of TIM-3 in TCGA sets
p<0.0001
Expression of PD-1 in TCGA sets
p=0.0003
(B)
DAPI/LAG-3/CD-4
DAPI/TIM-3/CD-3
DAPI/PD-1/CD-3
Brain
Glioblastoma
50μm
25μm
(C)
CD4+ LAG-3+ cell counts
CD3+ TIM-3+ cell counts
CD3+ PD-1+ cell counts
p<0.05
Brain n = 6
Glioblastoma n = 30
(D)
DAPI/LAG-3/CD4
Case 1
HLA-DP
HLA-DQ
100μm
25μm
(E)
Low expression of HLA-DP
High expression of HLA-DP
p=0.0516
n = 30
Low expression of HLA-DQ
High expression of HLA-DQ
p=0.5266
n = 30
CD4+LAG-3+ cell counts
(F)
p=0.0594, r=0.3481, n = 30
p=0.4093, r=0.1564, n = 30
HLA-DP IHC scores
HLA-DQ IHC scores
LAG-3+CD4+ cell counts
(G)
Overall survival (n = 46)
HLA-DPLow LAG-3Low
HLA-DPHigh LAG-3High
p=0.0633
Others
Survival
Survival time (months)
(H)
HLA-DQLow LAG-3Low
HLA-DQHigh LAG-3High
p=0.2518
(I)
HLA-DPLOW and LAG-3LOW
p=0.0274

TABLE 2 Correlations among human leukocyte antigen (HLA)-DP, HLA-DQ, lymphocyte-activation gene 3 (LAG-3), and interleukin-10 (IL-10) levels in glioblastoma.

	HLA-DP				HLA-DQ				LAG-3			
	High	Low	*r*	*p* value	High	Low	*r*	*p* value	High	Low	*r*	*p* value
LAG-3			0.3507	<0.05*			0.3107	<0.05*			–	–
High	19	7	–	–	18	8	–	–	–	–	–	–
Low	13	12	–	–	13	12	–	–	–	–	–	–
IL-10			0.299	<0.05*			0.313	<0.05*			0.3935	<0.05*
High	16	5	–	–	14	7	–	–	16	5	–	–
Low	16	14	–	–	17	13	–	–	10	20	–	–

*$p < 0.05$ indicates statistically significant difference.

numbers of LAG-3^{high}IL-10^{high} or LAG-3^{low}IL-10^{low} are shown in Table 2. Patients with LAG-3^{High}IL-10^{High} had shorter OS than those with LAG-3^{Low}IL-10^{Low} (Figure 4D). According to combined expression of HLA-II, LAG-3, and IL-10 in paraffin-embedded GBM specimens, multivariate analysis indicated that patients with HLA-II^{High}LAG-3^{High}IL-10^{High} had a worse OS (Figure 4E,F). Patients with HLA-II^{+}IL-10^{+} associated with increased LAG-3^{+} T cell infiltration synergistically leads to poor prognosis. We established an in vivo subcutaneous GBM tumor model using brain GL261 tumor cells, and treated the tumor-bearing mice with anti-LAG-3 and IL-10 (Figure 4G). We found anti-LAG-3 and IL-10 combined treatment significantly inhibited tumor growth compared to anti-LAG-3 or anti-IL-10 alone (Figure 4H,I). Combined anti-LAG-3 and anti-IL-10 inhibition significantly decreased the tumor weight compared to anti-LAG-3 or anti-IL-10 alone (Figure 4J). Furthermore, immunofluorescence staining analysis showed that combined anti-LAG-3 and anti-IL-10 also reduced $CD4^{+}$LAG-3^{+} (Figure 4K,L) and $CD8^{+}$LAG-3^{+} cell infiltration in tumor tissues (Figure 4M,N). Therefore, blocking of LAG-3 and IL-10 might be beneficial for improving the clinical outcome of GBM patients.

3.5 | TNF-$\alpha^{+}CD68^{+}$ macrophage infiltration associated with HLA-II upregulation in GBM

Based on TCGA, we analyzed the immune infiltration patterns according to the HLA-II scores in GBM using ssGSEA. Heat map analysis revealed that the expression of HLA-II was positively correlated with the infiltration of macrophages and neutrophils, and immune checkpoint molecules (Figure S9).

To explore whether infiltration of immune cells contributes to HLA-II upregulation in GBM, we measured the relationship between HLA-II expression and macrophage infiltration in 51 paraffin-embedded GBM specimens. Positive expression of CD68 and TNF-α associated with HLA-DP, HLA-DQ, and HLA-DR was observed in the same field of GBM (Figure 5A). Tumor necrosis factor-α expression and $CD68^{+}$ macrophage infiltration were higher in GBM specimens than in control specimens (Figure 5B,C). Increased $CD68^{+}$ macrophage infiltration positively correlated with TNF-α upregulation in GBM samples (Figure 5D). Increased TNF-α expression was also positively correlated with $CD68^{+}$ macrophage infiltration and HLA-II upregulation (Figure 5E–G). $CD68^{+}$ macrophage infiltration was positively correlated with HLA-II upregulation (Figure 5H,I). These results suggest that $CD68^{+}$ macrophages expressing TNF-α could be related to HLA-II upregulation in GBM.

Based on immunofluorescence staining in 30 frozen GBM specimens, the relationship between TNF-$\alpha^{+}CD68^{+}$ macrophage infiltration and HLA-II expression was further investigated. Tumor necrosis factor-α and CD68 colocalization was observed in the GBM stroma, which was associated with HLA-DP and HLA-DQ expression in the same field (Figures 5K and S10A). The increased number of TNF-$\alpha^{+}CD68^{+}$ macrophages was correlated with HLA-II upregulation in GBM specimens (Figure 5L,M). These results indicate that $CD68^{+}$ macrophages producing TNF-α could contribute to HLA-II upregulation in GBM. We also detected IL-10 expression in Arg-1^{+} M2 macrophages in frozen GBM stroma. Immunofluorescence staining showed the infiltration of Arg-1^{+} M2 (Figure S10B,C) and the number of IL-10^{+}Arg-1^{+} macrophages (Figure S10D,E) was increased in GBM stroma. Thus, M2 macrophages infiltrated the GBM stroma, and might also contribute to IL-10 upregulation.

FIGURE 3 Human leukocyte antigen-II (HLA-II) molecules are related to the expression of interleukin-10 (IL-10) in glioblastoma (GBM). (A) Based on the RT-PCR results of 21 pairs of fresh tumor tissues, the expression of HLA-DP was upregulated in 13 cases of GBM, and HLA-DQ was upregulated in 14 cases of GBM. (B, C) GBM cases were divided into HLA-II upregulation and HLA-II downregulation groups. The expression of IL-10, transforming growth factor-β (TGF-β), and prostaglandin E2 (PGE2) in fresh GBM samples was compared between those two groups ($p < 0.05$). (D) Representative immunohistochemical (IHC) images show the expression of IL-10 in paraffin-embedded GBM specimens. (E) Expression of IL-10 was compared between GBM and control specimens ($p < 0.001$). (F) Survival outcomes of patients were shown according to the expression of IL-10 in paraffin GBM specimens. (G) Representative IHC images indicate the expression of HLA-DP, HLA-DQ, and IL-10 in paraffin GBM specimens. (H, I) Spearman's correlation analysis indicates the relationship between the expression of HLA-II and IL-10 in paraffin GBM specimens ($n = 51$). (J, K) Survival outcomes of patients were shown according to both HLA-II and IL-10 expression in paraffin GBM specimens, HLA-II^{Low}IL-10^{Low} versus HLA-II^{High}IL-10^{High} ($n = 46$). N, Normal control brain; T, Tumor.

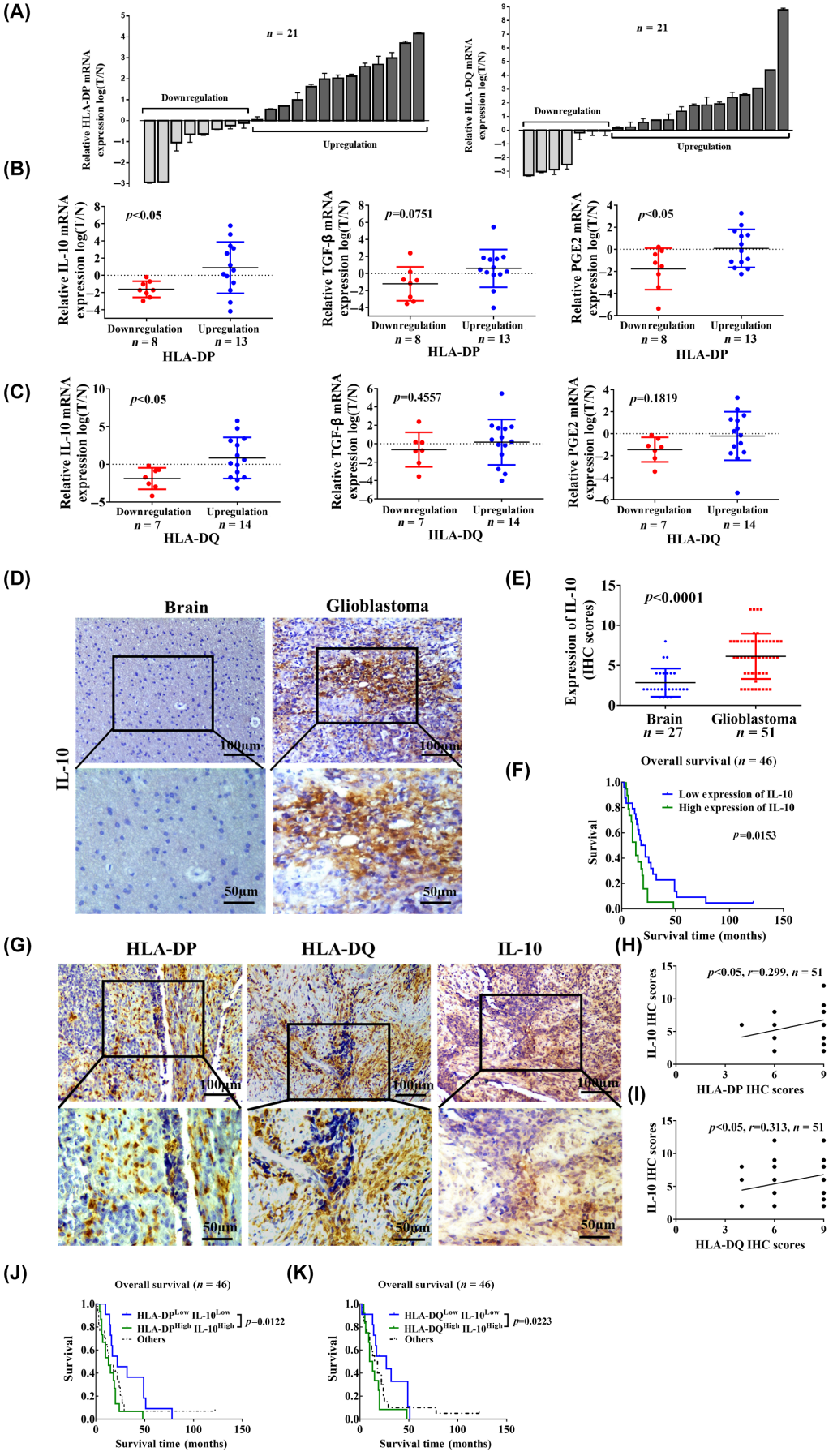
(A)
Relative HLA-DP mRNA expression log(T/N)
n = 21
Downregulation
Upregulation
Relative HLA-DQ mRNA expression log(T/N)
n = 21
Downregulation
Upregulation
(B)
Relative IL-10 mRNA expression log(T/N)
p<0.05
Downregulation n = 8
Upregulation n = 13
HLA-DP
Relative TGF-β mRNA expression log(T/N)
p=0.0751
Downregulation n = 8
Upregulation n = 13
HLA-DP
Relative PGE2 mRNA expression log(T/N)
p<0.05
Downregulation n = 8
Upregulation n = 13
HLA-DP
(C)
Relative IL-10 mRNA expression log(T/N)
p<0.05
Downregulation n = 7
Upregulation n = 14
HLA-DQ
Relative TGF-β mRNA expression log(T/N)
p=0.4557
Downregulation n = 7
Upregulation n = 14
HLA-DQ
Relative PGE2 mRNA expression log(T/N)
p=0.1819
Downregulation n = 7
Upregulation n = 14
HLA-DQ
(D)
Brain
Glioblastoma
IL-10
100μm
50μm
(E)
Expression of IL-10 (IHC scores)
p<0.0001
Brain n = 27
Glioblastoma n = 51
(F)
Overall survival (n = 46)
Low expression of IL-10
High expression of IL-10
p=0.0153
Survival
Survival time (months)
(G)
HLA-DP
HLA-DQ
IL-10
100μm
50μm
(H)
IL-10 IHC scores
p<0.05, r=0.299, n = 51
HLA-DP IHC scores
(I)
IL-10 IHC scores
p<0.05, r=0.313, n = 51
HLA-DQ IHC scores
(J)
Overall survival (n = 46)
HLA-DPLow IL-10Low
HLA-DPHigh IL-10High
p=0.0122
Others
Survival
Survival time (months)
(K)
Overall survival (n = 46)
HLA-DQLow IL-10Low
HLA-DQHigh IL-10High
p=0.0223
Others
Survival
Survival time (months)

3.6 | Tumor necrosis factor-α upregulating HLA-II expression contributes to GBM progression

To further confirm that macrophages secrete TNF-α to upregulate the expression of HLA-II in GBM cells, human GBM U87 and U251 cell lines were used as in vitro models. After stimulation with TNF-α for 24 h, we detected HLA-II expression in human GBM cells by FCM staining and western blot analysis. Flow cytometry analysis indicated TNF-α increased HLA-II expression in U87 and U251 cells (Figure 6A,B). Western blot results showed the expression of HLA-DP and HLA-DQ was significantly upregulated in GBM cells treated with TNF-α (Figure 6C,D). Human monocyte THP-1 cells were cultured and differentiated into M1-type macrophages, the supernatant was then collected to stimulate the U87 and U251 cells. Supernatants from M1-type THP-1 macrophages upregulated the expression of HLA-DP and HLA-DQ in tumor cells (Figure 6E,F). Inhibiting TNF-α in the medium from M1-type THP-1 cells prevented the upregulation of HLA-DP and HLA-DQ in tumor cells (Figure 6G,H). These results indicate that macrophages secreting TNF-α upregulate HLA-II expression in GBM cells.

We established AN in vivo subcutaneous GBM tumor model using brain GL261 tumor cells, and treated the tumor-bearing mice with sTNFR:Fc fusion protein to block TNF-α (Figure S11A). We found sTNFR:Fc treatment significantly inhibited tumor growth (Figure S11B–D). Immunofluorescence staining analysis showed sTNFR:Fc decreased mouse MHC-II (IAIE) expression in tumor tissues (Figure S11E,F). In addition, blocking TNF-α also reduced $CD4^+LAG\text{-}3^+$ cell infiltration in tumor tissues (Figure S11G,H). Therefore, the results support that TNF-α-dependent inflammation contributes to GBM progression by upregulating HLA-II.

4 | DISCUSSION

Given the extensive heterogeneity of glioma cells, it has proven difficult to develop small-molecule inhibitors for GBM because blocking a single oncogenic signaling pathway might not be sufficient to induce tumor apoptosis.[28] The current understanding of the immune microenvironment of gliomas is gradually improving and the central nervous system immune system is no longer considered an "immune-privileged" site.[29,30] Blockade of PD-1 has shown significant efficacy in improving the survival of patients with melanoma brain metastases[31]; however, ICI immunotherapy options for GBM require continued development, despite the failure of PD-1 blockade in patients.[32] In terms of the diversity of ICI systems in GBM, several receptor–ligand systems, such as PD-1–PD-L1, TIM-3–galectin-9, and LAG-3–MHC-II, could act in combination to inhibit T cell-mediated immunity.[28] Therefore, this study mainly focused on T cell–tumor cell interactions, LAG-3–MHC-II, in human GBM, which could reveal additional inhibitory strategies for immunotherapy.

The MHC-II of APCs, such as macrophages, dendritic cells, or B cells, present antigenic peptides to $CD4^+$ T cells, which are central to adaptive immune responses.[33] However, tumor cells with MHC-II expression and lower levels of Th1 cytokines showed resistance to anti-PD-1.[21] This study supports that expression of MHC-II in cancer cells, nonspecific APCs, are related to T cell exhaustion in the tumor environment.[34] Abnormal expression of HLA-DR promoted the migration and invasion of melanoma cells[27] and caused tumor escape by recruiting inflammatory tumor antigen-specific $CD4^+$ T cells.[35] In this study, we analyzed the expression of HLA-II based on TCGA and clinical specimens. Using immunofluorescence staining and FCM analysis, we clearly observed that HLA-II expression was increased in $GFAP^+$ GBM cells. Human leukocyte antigen II was highly expressed in human GBM and correlated with $CD4^+$ T cell infiltration in the GBM microenvironment. High levels of HLA-II in tumor cells have been associated with increased intratumoral $CD4^+$ T cell density, whereas tumor MHC-II-stimulated $CD4^+$ T cell subsets show dysfunctions in immunity.[36,37] Therefore, $HLA\text{-}II^+$ GBM might be related to $CD4^+$ T cell exhaustion.

Lymphocyte-activation gene 3, an early marker of T cell exhaustion, is expressed in TILs and tumor-associated perivascular lymphocytes in human GBM.[16] The combination of anti-LAG-3 with PD-1 inhibitor achieved better treatment outcomes in a mouse glioma model.[8] The inhibition of $CD4^+$ T cell activation through LAG-3 is dependent on stable pMHC-II recognition.[8] Major histocompatibility complex-II interacts with LAG-3 through residues on the membrane-distal region, the top face of the LAG-3 D1 domain.[38] Mair et al. reported LAG-3 was rarely expressed on TILs in human GBM by scoring cell density,[39] while Harris-Bookman et al. observed higher expression of LAG-3 in GBM, in which 66% of GBM samples showed variable LAG-3 expression on perivascular lymphocytes.[16] In our study, LAG-3, TIM-3, and PD-1 quantification was calculated

FIGURE 4 Targeting of lymphocyte-activation gene 3 (LAG-3) and interleukin-10 (IL-10) inhibits glioblastoma (GBM) progression. (A) Based on the immunohistochemical (IHC) staining in paraffin GBM specimens, the correlation between $LAG\text{-}3^+$ cell number and IL-10 expression is shown ($n = 51$). (B, C) The number of $LAG\text{-}3^+$ cells in patients with human leukocyte antigen-II $(HLA\text{-}II)^{High}IL\text{-}10^{High}$ was compared to that in patients with $HLA\text{-}II^{Low}IL\text{-}10^{Low}$ ($n = 51$). (D) Survival outcomes of patients are shown according to both LAG-3 and IL-10 expression in paraffin-embedded GBM specimens, $LAG\text{-}3^{Low}IL\text{-}10^{Low}$ versus $LAG\text{-}3^{High}IL\text{-}10^{High}$ ($n = 46$). (E, F) Survival outcomes of patients are shown according to combined expression of HLA-II, LAG-3, and IL-10 together in paraffin-embedded GBM specimens, $HLA\text{-}II^{Low}LAG\text{-}3^{Low}IL\text{-}10^{Low}$ versus $HLA\text{-}II^{High}LAG\text{-}3^{High}IL\text{-}10^{High}$ ($n = 46$). (G) Schematic of experimental design. (H) Images of tumors from control, anti-IL-10, anti-LAG-3, and anti-IL-10 + LAG-3 groups are shown at day 22 after injection. (I) Tumor volumes were measured every 2 days from day 12 to 22. Data are shown as mean ± SD ($n = 4$). (J) Tumor weights were measured at day 22. Data are shown as mean ± SD ($n = 4$). (K, M) Immunofluorescence staining indicated that $CD4^+LAG\text{-}3^+$ and $CD8^+LAG\text{-}3^+$ cells were infiltrated in the tumor tissues. White arrows show colocalized cells. (L, N) Data are shown as mean ± SD ($n = 4$). $^*p < 0.05$. Con, control; TNF-α, tumor necrosis factor-α.

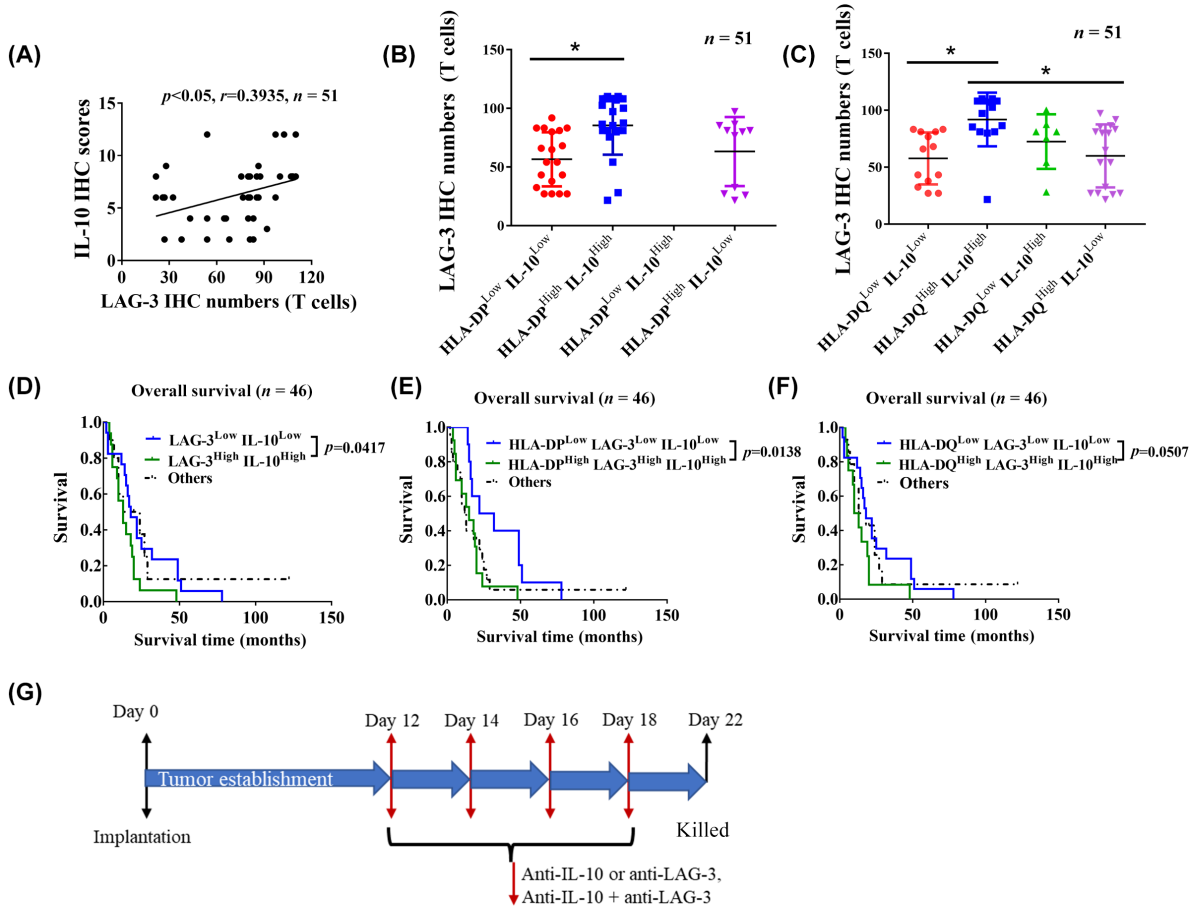
(A)
p<0.05, r=0.3935, n = 51
IL-10 IHC scores
LAG-3 IHC numbers (T cells)
(B)
n = 51
LAG-3 IHC numbers (T cells)
HLA-DP^Low IL-10^Low
HLA-DP^High IL-10^High
HLA-DP^Low IL-10^High
HLA-DP^High IL-10^Low
(C)
n = 51
HLA-DQ^Low IL-10^Low
HLA-DQ^High IL-10^High
HLA-DQ^Low IL-10^High
HLA-DQ^High IL-10^Low
(D)
Overall survival (n = 46)
LAG-3^Low IL-10^Low
LAG-3^High IL-10^High
Others
p=0.0417
Survival
Survival time (months)
(E)
Overall survival (n = 46)
HLA-DP^Low LAG-3^Low IL-10^Low
HLA-DP^High LAG-3^High IL-10^High
Others
p=0.0138
(F)
Overall survival (n = 46)
HLA-DQ^Low LAG-3^Low IL-10^Low
HLA-DQ^High LAG-3^High IL-10^High
Others
p=0.0507
(G)
Day 0
Day 12
Day 14
Day 16
Day 18
Day 22
Tumor establishment
Implantation
Killed
Anti-IL-10 or anti-LAG-3,
Anti-IL-10 + anti-LAG-3

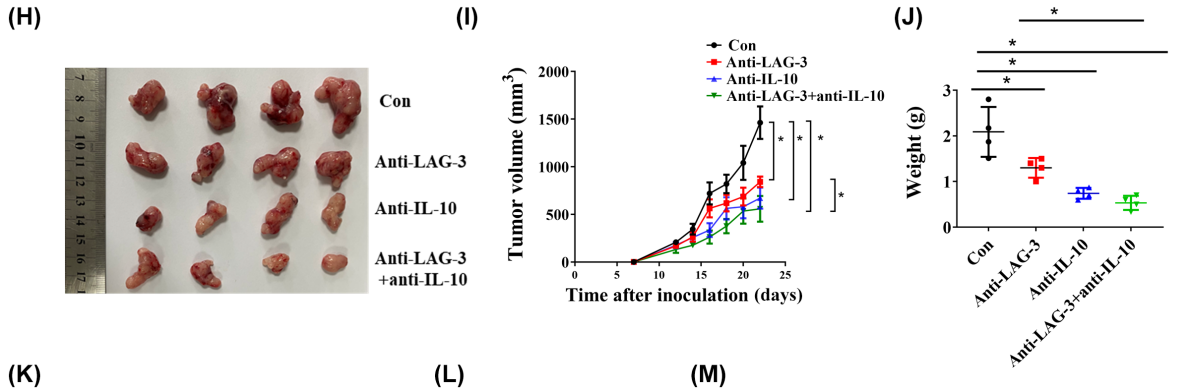
(H)
Con
Anti-LAG-3
Anti-IL-10
Anti-LAG-3
+anti-IL-10
(I)
Con
Anti-LAG-3
Anti-IL-10
Anti-LAG-3+anti-IL-10
Tumor volume (mm^3)
Time after inoculation (days)
(J)
Weight (g)
Con
Anti-LAG-3
Anti-IL-10
Anti-LAG-3+anti-IL-10

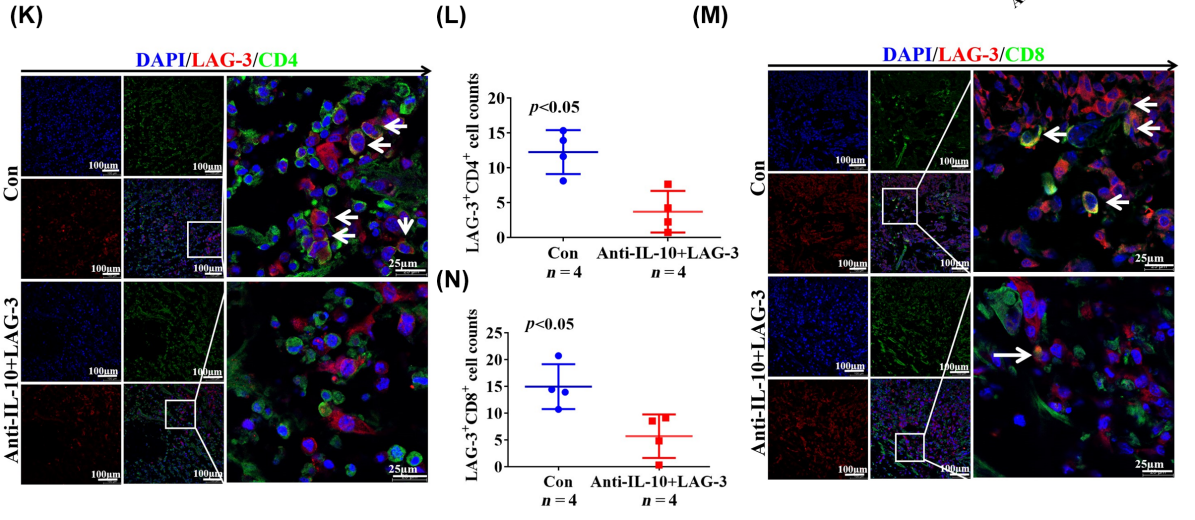
(K)
DAPI/LAG-3/CD4
Con
Anti-IL-10+LAG-3
(L)
p<0.05
LAG-3^+CD4^+ cell counts
Con
n = 4
Anti-IL-10+LAG-3
n = 4
(N)
p<0.05
LAG-3^+CD8^+ cell counts
Con
n = 4
Anti-IL-10+LAG-3
n = 4
(M)
DAPI/LAG-3/CD8
Con
Anti-IL-10+LAG-3

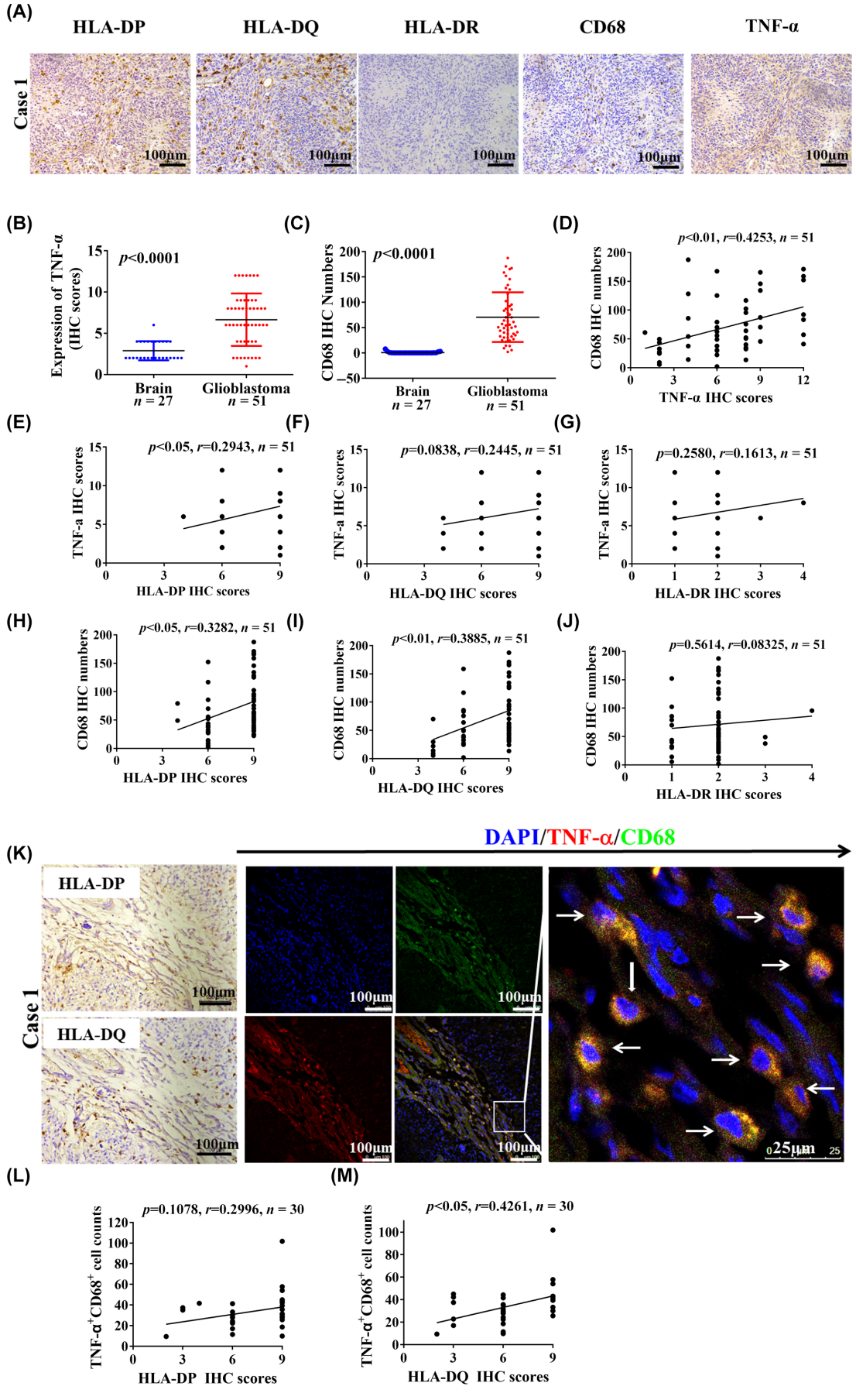
(A)
HLA-DP
HLA-DQ
HLA-DR
CD68
TNF-α
Case 1
100μm
(B)
Expression of TNF-α (IHC scores)
p<0.0001
Brain n = 27
Glioblastoma n = 51
(C)
CD68 IHC Numbers
p<0.0001
Brain n = 27
Glioblastoma n = 51
(D)
p<0.01, r=0.4253, n = 51
CD68 IHC numbers
TNF-α IHC scores
(E)
p<0.05, r=0.2943, n = 51
TNF-a IHC scores
HLA-DP IHC scores
(F)
p=0.0838, r=0.2445, n = 51
TNF-a IHC scores
HLA-DQ IHC scores
(G)
p=0.2580, r=0.1613, n = 51
TNF-a IHC scores
HLA-DR IHC scores
(H)
p<0.05, r=0.3282, n = 51
CD68 IHC numbers
HLA-DP IHC scores
(I)
p<0.01, r=0.3885, n = 51
CD68 IHC numbers
HLA-DQ IHC scores
(J)
p=0.5614, r=0.08325, n = 51
CD68 IHC numbers
HLA-DR IHC scores
(K)
DAPI/TNF-α/CD68
HLA-DP
HLA-DQ
Case 1
100μm
25μm
(L)
p=0.1078, r=0.2996, n = 30
TNF-α+CD68+ cell counts
HLA-DP IHC scores
(M)
p<0.05, r=0.4261, n = 30
TNF-α+CD68+ cell counts
HLA-DQ IHC scores

FIGURE 5 Tumor necrosis factor-α (TNF-α)$^{+}$CD68^{+} macrophage infiltration is associated with human leukocyte antigen-II (HLA-II) upregulation in glioblastoma (GBM). (A) Representative immunohistochemical (IHC) images indicate the expression of HLA- II, TNF-α, and CD68 in the same field in paraffin-embedded GBM samples. (B, C) Expression of TNF-α and the CD68^{+} macrophage infiltration were compared between GBM and control specimens ($p < 0.05$). (D) Based on the IHC staining in paraffin-embedded GBM samples, the correlation between CD68^{+} macrophage infiltration and TNF-α expression is shown ($n = 51$). (E–G) Correlation between TNF-α expression and HLA-II expression ($n = 51$). (H–J) Correlation between CD68^{+} macrophage infiltration and HLA-II expression ($n = 51$). (K) Immunofluorescence staining shows that TNF-α and CD68 is colocalized in the tumor stroma, which is associated with HLA-DP and HLA-DQ expression in the same field. White arrows indicate colocalized cells. (L, M) Based on immunofluorescence staining of TNF-α and CD68, the correlation between the number of infiltrated TNF-α^{+}CD68^{+} cells and HLA-II expression is shown ($n = 30$).

by counting the number of positive lymphocytes per high-powered field of view. Here, the infiltration of LAG-3^{+}, TIM-3^{+}, and PD-1^{+} cells in GBM stroma was more than those in the controls. Lymphocyte-activation gene 3 was mostly expressed in the GBM stroma, not in tumor cells or macrophages. In addition, increased CD4^{+}LAG-3^{+} T cell infiltration in GBM stroma was confirmed by LAG-3 and CD4 colocalization in the tumor stroma by immunofluorescence staining, which are consistent with Harris-Bookman et al.'s findings. Although LAG-3 or MHC-II expression was not associated with OS, the combination of HLA-DQ^{High} and LAG-3^{High} was associated with poor OS in GBM patients. A previous study showed that MHC-II^{+} tumors with increased LAG-3 expression suppress MHC-II-mediated antigen presentation, which preferentially results in acquired resistance to PD-1 therapy.[14] Therefore, interactions between LAG-3 and MHC-II might confer an immunosuppressive environment in GBM patients. Interference of the LAG-3–MHC-II interaction could be a potential therapeutic target for GBM.

T cell activation requires antigen recognition by MHC molecules binding to T cell receptors (signal 1), costimulatory signaling (signal 2), and cytokine priming (signal 3).[40,41] Cytokines have received more attention as important predictive biomarkers for prognosis and adverse reactions to ICI therapy. Immunosuppressive cytokines, such as IL-10, PEG2, and TGF-β, are produced by immune cells and tumor cells, impairing the efficiency of ICI therapy.[42–45] In this study, the upregulation of IL-10, PEG2, and TGF-β was observed in GBM. Interleukin-10^{+}Arg-1^{+} macrophages were increased in GBM stroma compared to that in the controls, suggesting M2 macrophages were also an important producer of IL-10 in GBM. Interleukin-10 plays crucial immunosuppressive roles, promoting tumor progression and immune evasion in GBM.[44] Interleukin-10 has broad immunosuppressive functions through the downstream STAT3 pathway and inhibits APC-mediated T cell activation, directly causing CD4^{+} T cell anergy.[46] An IL-10 inhibitor was shown to generate a T cell-mediated carcinoma cell death, which was reversed by MHC-II blockade, confirming the essential role of MHC-II in IL-10-induced CD4^{+} T cell dysfunction in the tumor environment.[47] In this study, HLA-II upregulation and increased number of LAG-3^{+} cells in the GBM stroma were also positively correlated with IL-10 upregulation in GBM, and the combination of IL-10^{High} and HLA-II^{High} was associated with poor OS in patients. A combination of IL-10 and IL-35 has been shown to induce LAG-3 expression in memory T cells, dampening the immune response.[48] Our study showed that an increased number of LAG-3^{+} cells in the GBM stroma was also positively correlated with IL-10 upregulation. Glioblastoma with HLA-II^{High}IL-10^{High} showed increased LAG-3^{+} T cell infiltration, which synergistically led to poor prognosis in patients. Therefore, IL-10 might be a strong factor in promoting MHC-II–LAG-3-induced CD4^{+} T cell exhaustion. To show direct evidence that targeting of the LAG-3–HLA-II axis and IL-10 could be beneficial in immunotherapy in GBM patients, we established an in vivo therapeutic model using anti-LAG-3 and anti-IL-10 Ab. We found combined anti-LAG-3 and IL-10 treatment significantly inhibited tumor growth in tumor-bearing mice. Furthermore, combined anti-LAG-3 and anti-IL-10 also reduced CD4^{+}LAG-3^{+} and CD8^{+}LAG-3^{+} cell infiltration in tumor tissues. Human leukocyte antigen-II comprises multiple MHC-II isotypes in humans, which are critical for antigen presentation to CD4^{+} T lymphocytes, not for CD8^{+} T cells.[40,41] Except for CD4^{+}LAG-3^{+} cells, we found CD8^{+}LAG-3^{+} cell infiltration was increased in human GBM tissues. However, the number of CD8^{+}LAG-3^{+} cells was not correlated with HLA-II expression. Interleukin-10, an important immunosuppressive cytokine, plays a critical role in CD8^{+} T cell exhaustion by promoting inhibitory receptor expression (PD-1, TIM-3, and LAG-3).[49] Blocking LAG-3–IL-10 could inhibit CD4^{+} and CD8^{+} T cell exhaustion, which contributes to antitumor efficacy. Human leukocyte antigen-II on the surface of tumor-associated IL-10 might be sufficient to induce CD4^{+} T cell suppression through LAG-3 in GBM. Thus, targeting these pathways could be beneficial for improving the clinical outcome of GBM patients.

The immune infiltration patterns associated with HLA-II expression in GBM were analyzed using ssGSEA. The expression of HLA-II is positively correlated with macrophages and neutrophils. In GBM, the most abundant stromal cell type is macrophages, which can comprise more than 30% of infiltrating cells[50,51]; the majority (80%) of GBM-associated macrophages differentiates from recruited bone marrow macrophages. Macrophages adjust their phenotype and function according to the local microenvironment and participate in tumor development.[52,53] Increased macrophage recruitment to the tumor area induces epithelial cell activation by secreting TNF-α, which contributes to tumor progression.[50] Serum levels of TNF-α are significantly enhanced in patients with GBM.[54] Macrophages and microglia in GBM are also major producers of TNF-α.[55] In the current study, we observed that TNF-α is not only expressed in GBM tumor cells but also in CD68^{+} macrophages in the tumor stroma. We recently discovered that TNF-α-dependent lung inflammation increases MHC-II expression in lung adenocarcinoma cells of AT-II cellular origin, contributing to regulatory T cell

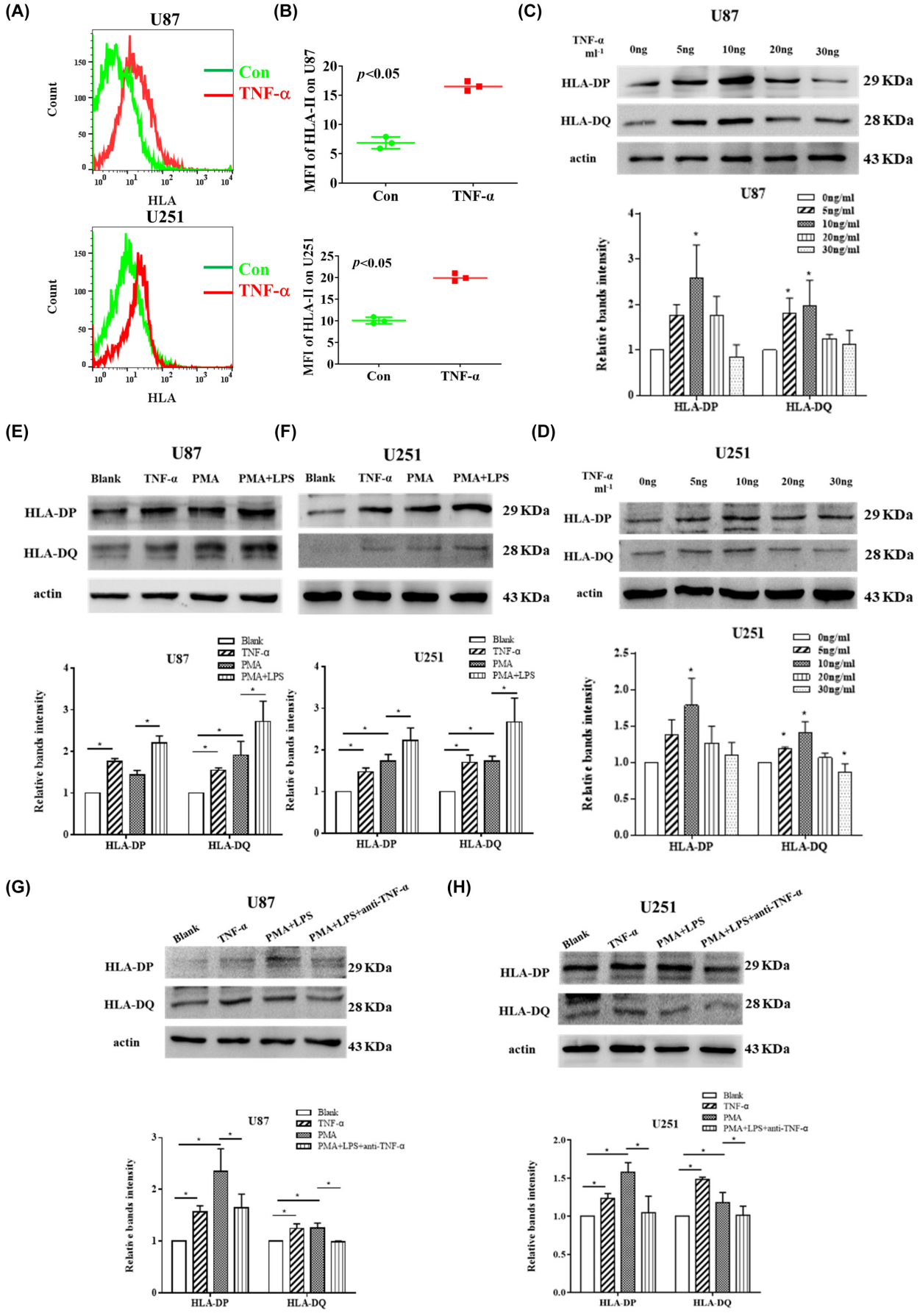
(A)
U87
Count
HLA
Con
TNF-α
U251
(B)
MFI of HLA-II on U87
p<0.05
Con
TNF-α
MFI of HLA-II on U251
(C)
U87
TNF-α ml-1
0ng
5ng
10ng
20ng
30ng
HLA-DP
HLA-DQ
actin
29 KDa
28 KDa
43 KDa
0ng/ml
5ng/ml
10ng/ml
20ng/ml
30ng/ml
Relative bands intensity
(E)
U87
Blank
TNF-α
PMA
PMA+LPS
(F)
U251
(D)
U251
(G)
U87
PMA+LPS+anti-TNF-α
PMA+LPS+anti-TNF-α
(H)
U251

FIGURE 6 THP-1 macrophages secreting tumor necrosis factor-α (TNF-α) upregulate the expression of human leukocyte antigen (HLA)-DP and HLA-DQ in U87 and U251 cells. (A, B) U87 and U251 cells were treated with 10 ng/mL TNF-α, and the expression of HLA-DP and HLA-DQ was measured by flow cytometry. Data were shown as mean ± SD ($n = 3$, $^*p < 0.05$ vs. Control [Con]). (C, D) U87 and U251 cells were treated with different doses of TNF-α, and the expression of HLA-DP and HLA-DQ was measured by western blot analysis. Data are shown as mean ± SD ($n = 3$, $^*p < 0.05$ vs. Con). (E, F) The supernatant from phorbol 12-myristate 13-acetate (PMA)-induced THP-1 (M0) and lipopolysaccharide (LPS)-activated PMA-induced THP-1 (M1) was collected to stimulate U87 and U251 cells, and the expression of HLA-DP and HLA-DQ were measured by western blot analysis. Data were shown as mean ± SD ($n = 3$, $^*p < 0.05$). (G, H) Anti-TNF-α neutralizing Ab was used to neutralize the TNF-α in the supernatant, and the expression of HLA-DP and HLA-DQ were measured by western blot. Data are shown as mean ± SD ($n = 3$, $^*p < 0.05$). The experiments were repeated three times. MFI, mean fluorescence intensity.

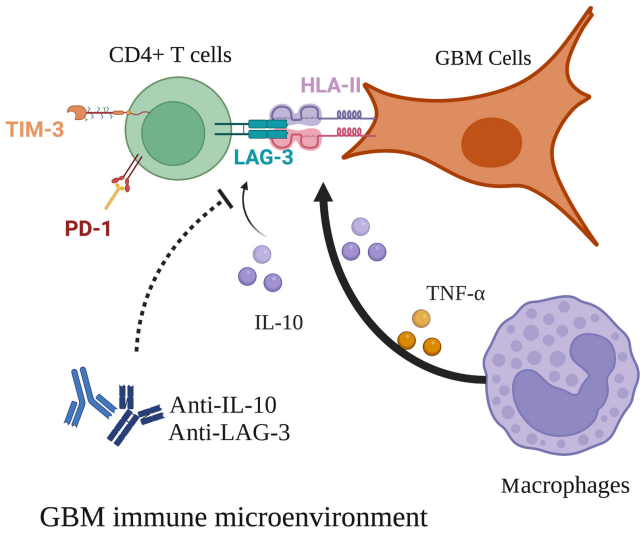

FIGURE 7 Macrophages in the tumor microenvironment upregulated human leukocyte antigen-II (HLA-II) expression in glioblastoma (GBM) cells through tumor necrosis factor-α (TNF-α). HLA-II interacted with lymphocyte-activation gene 3 (LAG-3) confers an immunosuppressive environment in GBM. Interleukin-10 (IL-10) could be a strong factor that promotes HLA-II–LAG-3-induced $CD4^+$ T cell exhaustion in GBM, leading to poor prognosis. PD-1, programmed cell death protein 1; TIM-3, T cell immunoglobulin domain and mucin domain-3.

expansion.[34] Tumor necrosis factor-α can mediate aberrant expression of MHC-II-like molecules in melanoma cells, thereby limiting the tumor-suppressive activity of $CD4^+$ T cells.[35] In this study, HLA-II expression in GBM was correlated with TNF-α^+CD68^+ macrophage infiltration in the stroma. Furthermore, mononuclear THP-1 cells secreted TNF-α, which could increase HLA-II expression in U87 and U251 cells in vitro. $CD68^+$ macrophages upregulate HLA-II expression in GBM cells through TNF-α. In order to address the contribution of TNF-α in GBM progression, we established an in vivo therapeutic model using sTNFR:Fc to neutralize TNF-α.[34] We found sTNFR:Fc treatment significantly inhibited tumor growth. In addition, blocking TNF-α decreased MHC-II expression in mice GBM tumor cells, and reduced $CD4^+LAG\text{-}3^+$ cell infiltration. These results indicate that TNF-α upregulating HLA-II expression contributes to GBM progression.

In conclusion, we found that HLA-II and IL-10 were highly expressed in GBM and correlated with increased $CD4^+LAG\text{-}3^+$ cell infiltration in the stroma. Patients with $HLA\text{-}II^+IL\text{-}10^+$ associated with increased $LAG\text{-}3^+$ T cell infiltration synergistically have poor prognosis. In addition, combined anti-LAG-3 and anti-IL-10 treatment inhibited tumor growth in a mouse brain GL261 tumor model. $CD68^+$ macrophages in the tumor microenvironment upregulated HLA-II expression in GBM cells through TNF-α. Blocking TNF-α-dependent inflammation inhibited tumor growth in a mouse GBM model. T cell–tumor cell interactions, LAG-3–HLA-II, could confer an immunosuppressive environment in GBM patients. Interleukin-10 could be a strong factor that promotes MHC-II–LAG-3-induced $CD4^+$ T cell exhaustion in GBM, leading to poor prognosis (Figure 7). This study provides new insights into targeting the LAG-3–MHC-II interaction that could be beneficial for improving the clinical outcomes of GBM patients.

AUTHOR CONTRIBUTIONS

Wenli Guo: Data curation; investigation; methodology; writing – original draft. **Daijun Peng:** Conceptualization; data curation; investigation; methodology; writing – original draft. **Yuee Liao:** Formal analysis; methodology. **Lei Lou:** Formal analysis; methodology. **Moran Guo:** Formal analysis; methodology. **Chen Li:** Formal analysis; resources. **Wangyang Yu:** Formal analysis; software. **Xiaoxi Tian:** Formal analysis; methodology. **Guohui Wang:** Formal analysis; software. **Ping Lv:** Conceptualization; investigation. **Jing Zuo:** Conceptualization; investigation. **Haitao Shen:** Conceptualization; data curation; funding acquisition; investigation; project administration; supervision; writing – original draft; writing – review and editing. **Yuehong Li:** Conceptualization; funding acquisition; investigation; project administration; supervision; writing – original draft; writing – review and editing.

ACKNOWLEDGMENTS

This work was supported by the National Natural Science Foundation of China (31570894; 81670939; 81672706), Natural Science Foundation of Hebei Province, China (H2019206709; H2021206351; H2022206551), and Science and Technology Program of Hebei Province, China (216Z7707G; 216Z7701G).

CONFLICT OF INTEREST STATEMENT

The authors declare no conflict of interest.

DATA AVAILABILITY STATEMENT

All data generated or analyzed during this study are included in this published article and its additional files. The analyzed datasets and used materials in the current study are available from the corresponding author on reasonable request.

ETHICS STATEMENT

Approval of the research protocol by an institutional review board: The study of human sample was approved by the Ethics Committee of Hebei Medical University, the Second Hospital, Hebei, China.

Informed consent: Informed consent was obtained from all patients in accordance with a protocol approved by the ethics review board of Hebei Medical University (approval no. 2019-R260). Written informed consent was obtained from each subject.

Registry and the registration no. of the study/trial: N/A.

Animal studies: Experimental protocols were approved by the Institutional Animal Care and Use Committee of Hebei Medical University. All animals were managed and treated according to the guidelines of Hebei Medical University.

ORCID

Wenli Guo https://orcid.org/0000-0003-4448-4601
Haitao Shen https://orcid.org/0000-0003-3111-0133

REFERENCES

1. Tan AC, Ashley DM, López GY, Malinzak M, Friedman HS, Khasraw M. Management of glioblastoma: state of the art and future directions[J]. *CA Cancer J Clin*. 2020;70(4):299-312.
2. Cloughesy TF, Mochizuki AY, Orpilla JR, et al. Neoadjuvant anti-PD-1 immunotherapy promotes a survival benefit with intratumoral and systemic immune responses in recurrent glioblastoma[J]. *Nat Med*. 2019;25(3):477-486.
3. Quail DF, Joyce JA. The microenvironmental landscape of brain tumors[J]. *Cancer Cell*. 2017;31(3):326-341.
4. Fu W, Wang W, Li H, et al. Single-cell atlas reveals complexity of the immunosuppressive microenvironment of initial and recurrent glioblastoma[J]. *Front Immunol*. 2020;11:835.
5. Broekman ML, Maas SLN, Abels ER, Mempel TR, Krichevsky AM, Breakefield XO. Multidimensional communication in the microenvirons of glioblastoma[J]. *Nat Rev Neurol*. 2018;14(8):482-495.
6. Wherry EJ, Kurachi M. Molecular and cellular insights into T cell exhaustion[J]. *Nat Rev Immunol*. 2015;15(8):486-499.
7. Kurachi M. CD8(+) T cell exhaustion[J]. *Semin Immunopathol*. 2019;41(3):327-337.
8. Maruhashi T, Okazaki IM, Sugiura D, et al. LAG-3 inhibits the activation of CD4(+) T cells that recognize stable pMHCII through its conformation-dependent recognition of pMHCII[J]. *Nat Immunol*. 2018;19(12):1415-1426.
9. Maruhashi T, Sugiura D, Okazaki IM, Okazaki T. LAG-3: from molecular functions to clinical applications[J]. *J Immunother Cancer*. 2020;8(2):e001014.
10. Huard B, Prigent P, Tournier M, Bruniquel D, Triebel F. CD4/major histocompatibility complex class II interaction analyzed with CD4- and lymphocyte activation gene-3 (LAG-3)-Ig fusion proteins[J]. *Eur J Immunol*. 1995;25(9):2718-2721.
11. Wang J, Sanmamed MF, Datar I, et al. Fibrinogen-like protein 1 is a major immune inhibitory ligand of LAG-3[J]. *Cell*. 2019;176:334-347.
12. Ascierto PA, Melero I, Bhatia S, et al. Initial efficacy of anti-lymphocyte activation gene-3 (anti–LAG-3; BMS-986016) in combination with nivolumab (nivo) in pts with melanoma (MEL) previously treated with anti–PD-1/PD-L1 therapy [M]. *Am Soc Clin Oncol*. 2017;35:9520.
13. Duhoux FP, Jager A, Dirix LY, et al. Combination of paclitaxel and a LAG-3 fusion protein (eftilagimod alpha), as a first-line chemoimmunotherapy in patients with metastatic breast carcinoma (MBC): final results from the run-in phase of a placebo-controlled randomized phase II [M]. *Am Soc Clin Oncol*. 2018;36:1050.
14. Johnson DB, Nixon MJ, Wang Y, et al. Tumor-specific MHC-II expression drives a unique pattern of resistance to immunotherapy via LAG-3/FCRL6 engagement[J]. *JCI Insight*. 2018;3(24):e120360.
15. Andrews LP, Somasundaram A, Moskovitz JM, et al. Resistance to PD1 blockade in the absence of metalloprotease-mediated LAG3 shedding[J]. *Sci Immunol*. 2020;5(49):eabc2728.
16. Harris-Bookman S, Mathios D, Martin AM, et al. Expression of LAG-3 and efficacy of combination treatment with anti-LAG-3 and anti-PD-1 monoclonal antibodies in glioblastoma[J]. *Int J Cancer*. 2018;143(12):3201-3208.
17. Lecocq Q, Keyaerts M, Devoogdt N, Breckpot K. The next-generation immune checkpoint LAG-3 and its therapeutic potential in oncology: third Time's a charm[J]. *Int J Mol Sci*. 2020;22(1):75.
18. Robinson J, Waller MJ, Fail SC, et al. The IMGT/HLA database[J]. *Nucleic Acids Res*. 2009;37:D1013-D1017.
19. Van Lith M, Mcewen-Smith RM, Benham AM. HLA-DP, HLA-DQ, and HLA-DR have different requirements for invariant chain and HLA-DM[J]. *J Biol Chem*. 2010;285(52):40800-40808.
20. Roemer MGM, Redd RA, Cader FZ, et al. Major histocompatibility complex class II and programmed death ligand 1 expression predict outcome after programmed death 1 blockade in classic Hodgkin lymphoma[J]. *J Clin Oncol*. 2018;36(10):942-950.
21. Johnson AM, Bullock BL, Neuwelt AJ, et al. Cancer cell-intrinsic expression of MHC class II regulates the immune microenvironment and response to anti-PD-1 therapy in lung adenocarcinoma[J]. *J Immunol*. 2020;204(8):2295-2307.
22. Johnson DB, Estrada MV, Salgado R, et al. Melanoma-specific MHC-II expression represents a tumour-autonomous phenotype and predicts response to anti-PD-1/PD-L1 therapy[J]. *Nat Commun*. 2016;7:10582.
23. Maclachlan BJ, Mason GH, Greenshields-Watson A, et al. Molecular characterization of HLA class II binding to the LAG-3 T cell co-inhibitory receptor[J]. *Eur J Immunol*. 2021;51(2):331-341.
24. Hemon P, Jean-Louis F, Ramgolam K, et al. MHC class II engagement by its ligand LAG-3 (CD223) contributes to melanoma resistance to apoptosis[J]. *J Immunol*. 2011;186(9):5173-5183.
25. Souri Z, Wierenga APA, Kroes WGM, et al. LAG3 and its ligands show increased expression in high-risk uveal melanoma[J]. *Cancers (Basel)*. 2021;13(17):4445.
26. Nagasaki J, Togashi Y, Sugawara T, et al. The critical role of CD4+ T cells in PD-1 blockade against MHC-II-expressing tumors such as classic Hodgkin lymphoma[J]. *Blood Adv*. 2020;4(17):4069-4082.
27. Costantini F, Barbieri G. The HLA-DR mediated signalling increases the migration and invasion of melanoma cells, the expression and lipid raft recruitment of adhesion receptors, PD-L1 and signal transduction proteins[J]. *Cell Signal*. 2017;36:189-203.
28. Marx S, Godicelj A, Wucherpfennig KW. A conceptual framework for inducing T cell-mediated immunity against glioblastoma[J]. *Semin Immunopathol*. 2022;44(5):697-707.
29. Yang K, Wu Z, Zhang H, et al. Glioma targeted therapy: insight into future of molecular approaches[J]. *Mol Cancer*. 2022;21(1):39.
30. Xu S, Tang L, Li X, Fan F, Liu Z. Immunotherapy for glioma: current management and future application[J]. *Cancer Lett*. 2020;476:1-12.
31. Bander ED, Yuan M, Carnevale JA, et al. Melanoma brain metastasis presentation, treatment, and outcomes in the age of targeted and immunotherapies[J]. *Cancer*. 2021;127(12):2062-2073.
32. Reardon DA, Brandes AA, Omuro A, et al. Effect of nivolumab vs bevacizumab in patients with recurrent glioblastoma: the CheckMate 143 phase 3 randomized clinical trial[J]. *JAMA Oncol*. 2020;6(7):1003-1010.
33. Unanue ER, Turk V, Neefjes J. Variations in MHC class II antigen processing and presentation in health and disease[J]. *Annu Rev Immunol*. 2016;34:265-297.
34. Guo N, Wen Y, Wang C, et al. Lung adenocarcinoma-related TNF-α-dependent inflammation upregulates MHC-II on alveolar type II

cells through CXCR-2 to contribute to Treg expansion[J]. *FASEB J*. 2020;34(9):12197-12213.
35. Donia M, Andersen R, Kjeldsen JW, et al. Aberrant expression of MHC class II in melanoma attracts inflammatory tumor-specific CD4+ T- cells, which dampen CD8+ T-cell antitumor reactivity[J]. *Cancer Res*. 2015;75(18):3747-3759.
36. Senosain MF, Zou Y, Novitskaya T, et al. HLA-DR cancer cells expression correlates with T cell infiltration and is enriched in lung adenocarcinoma with indolent behavior[J]. *Sci Rep*. 2021;11(1):14424.
37. Meyer S, Handke D, Mueller A, et al. Distinct molecular mechanisms of altered HLA class II expression in malignant melanoma[J]. *Cancers (Basel)*. 2021;13(15):3907.
38. Baixeras E, Huard B, Miossec C, et al. Characterization of the lymphocyte activation gene 3-encoded protein. A new ligand for human leukocyte antigen class II antigens[J]. *J Exp Med*. 1992;176(2):327-337.
39. Mair MJ, Kiesel B, Feldmann K, et al. LAG-3 expression in the inflammatory microenvironment of glioma[J]. *J Neuro-Oncol*. 2021;152(3):533-539.
40. Han Y, Xie W, Song D-G, Powell DJ Jr. Control of triple-negative breast cancer using ex vivo self-enriched, costimulated NKG2D CAR T cells[J]. *J Hematol Oncol*. 2018;11(1):92.
41. Qiao Y, Qiu Y, Ding J, et al. Cancer immune therapy with PD-1-dependent CD137 co-stimulation provides localized tumour killing without systemic toxicity[J]. *Nat Commun*. 2021;12(1):6360.
42. Wang M, Zhai X, Li J, et al. The role of cytokines in predicting the response and adverse events related to immune checkpoint inhibitors[J]. *Front Immunol*. 2021;12:670391.
43. Bertrand F, Montfort A, Marcheteau E, et al. TNFalpha blockade overcomes resistance to anti-PD-1 in experimental melanoma[J]. *Nat Commun*. 2017;8(1):2256.
44. Widodo SS, Dinevska M, Furst LM, Stylli SS, Mantamadiotis T. IL-10 in glioma[J]. *Br J Cancer*. 2021;125:1466-1476.
45. Lee JM, Tsuboi M, Kim ES, Mok TSK, Garrido P. Overcoming immunosuppression and pro-tumor inflammation in lung cancer with combined IL-1beta and PD-1 inhibition[J]. *Future Oncol*. 2022;18(27):3085-3100.
46. Saraiva M, Vieira P, O'Garra A. Biology and therapeutic potential of interleukin-10[J]. *J Exp Med*. 2020;217(1):e20190418.
47. Sullivan KM, Jiang X, Guha P, et al. Blockade of interleukin 10 potentiates antitumour immune function in human colorectal cancer liver metastases[J]. *Gut*. 2022;72:325-337.
48. Koga MM, Engel A, Pigni M, et al. IL10- and IL35-secreting MutuDC lines act in cooperation to inhibit memory T cell activation through LAG-3 expression[J]. *Front Immunol*. 2021;12:607315.
49. Sawant DV, Yano H, Chikina M, et al. Adaptive plasticity of IL-10+ and IL-35+ Treg cells cooperatively promotes tumor T cell exhaustion[J]. *Nat Immunol*. 2019;20(6):724-735.
50. Wei Q, Singh O, Ekinci C, et al. TNFalpha secreted by glioma associated macrophages promotes endothelial activation and resistance against anti-angiogenic therapy[J]. *Acta Neuropathol Commun*. 2021;9(1):67.
51. Gabrusiewicz K, Rodriguez B, Wei J, et al. Glioblastoma-infiltrated innate immune cells resemble M0 macrophage phenotype[J]. *JCI Insight*. 2016;1(2):e85841.
52. Orecchioni M, Ghosheh Y, Pramod AB, Ley K. Macrophage polarization: different gene signatures in M1(LPS+) vs. classically and M2(LPS-) vs. alternatively activated macrophages[J]. *Front Immunol*. 2019;10:1084.
53. Dan H, Liu S, Liu J, et al. RACK1 promotes cancer progression by increasing the M2/M1 macrophage ratio via the NF-κB pathway in oral squamous cell carcinoma[J]. *Mol Oncol*. 2020;14(4):795-807.
54. Albulescu R, Codrici E, Popescu ID, et al. Cytokine patterns in brain tumour progression[J]. *Mediat Inflamm*. 2013;2013:979748.
55. Meisen WH, Wohleb ES, Jaime-Ramirez AC, et al. The impact of macrophage- and microglia-secreted TNFalpha on oncolytic HSV-1 therapy in the glioblastoma tumor microenvironment[J]. *Clin Cancer Res*. 2015;21(14):3274-3285.

SUPPORTING INFORMATION

Additional supporting information can be found online in the Supporting Information section at the end of this article.

How to cite this article: Guo W, Peng D, Liao Y, et al. Upregulation of HLA-II related to LAG-3^{+}CD4^{+} T cell infiltration is associated with patient outcome in human glioblastoma. *Cancer Sci*. 2024;115:1388-1404. doi:10.1111/cas.16128